

Monitoring The HRC-S UV Rate: Observations of Vega

Deron Pease, Vinay Kashyap, Jeremy Drake and Michael Juda

10 May 2005

Abstract

We present an interim report on *Chandra* HRC-S calibration observations of Vega, an X-ray-dark and UV-bright star. The purpose of the observations is to monitor the UV response of the detector, and recently it has acquired further importance as a means to track the effects of increased radiation dosage on the UV/ion-shield of the detector. We find no conclusive evidence that leaving the HRC door open during radiation-zone passage is adversely affecting the UVIS. In order to spot any degradation early, we recommend continuing the higher frequency schedule of observations.

1 Introduction

Vega (α Lyr, $d = 7.76$ pc) is the closest and optically brightest single A0 V star in the sky. Though it produces copious UV photons, it is X-ray dark.¹ Therefore, any detection by the HRC-S of photons from Vega is a measurement of the HRC-S UV response. Furthermore, Vega is a very stable UV source, such that changes observed in the HRC-S response would indicate changes in the UV/ion-shield (UVIS) transmission. Here we present an analysis of the *Chandra* HRC-S in-flight calibration observations of Vega obtained over various spots on the detector array.

The HRC-S is equipped with aluminum-coated polyimide transmission filters designed to block UV rays from the MCP detectors. The thickness of the filter varies over the detector, ranging from a 2750Å-thick slab of polyimide coated with 786Å-thick layer of Al over a 'T'-shaped region covering the aimpoint, to a thinner 307Å layer of Al over the rest of the inner segment, and a thin 2090Å slab of polyimide coated with a 304Å layer of Al over the outer MCPs. As part of the *Chandra* in-flight calibration program, beginning in fall 1999 Vega has been observed by the HRC-S in imaging mode to monitor its UV response at the nominal aimpoint, at $\pm 10'$ off-axis on the central MCP, and at $\pm 20'$ off-axis on the wing MCPs.

In October 2003 the decision was made to stop moving the HRC door after the failure of the Y-shutter-motor select relay (see Juda 2004a). An identical relay is used to select the HRC door-motor for operation, and the failure of that relay with the door blocking the instrument would lead at least to a temporary loss of the use of the HRC. The draw-back to this decision is that the HRC is exposed to the flux of low-energy protons that scatter off the HRMA during radiation zone passages; these are the same low-energy protons that led to the early-mission CTI degradation in ACIS. While no known damage mechanism to the HRC has been identified due to the added radiation exposure, it

¹The two ways in which single main-sequence stars are thought to produce X-rays are 1) shock-heated regions in radiatively-driven hot stellar winds – common for O and early B stars – and 2) hot coronae sustained by dynamo-driven magnetic activity that arises in stars with convective envelopes – common for stars later than $\sim A7$. Vega is incapable of sustaining either of these X-ray producing mechanisms.

is possible that the low-energy protons stopping in the UVIS could cause the polyimide to become brittle and leading to cracks in the deposited aluminum film. A higher frequency schedule of HRC-S observations of Vega was started in 2004 to assess the impact of this action.

In this memo we present an analysis of all the observations of Vega to date at the above detector locations on the HRC-S (see §2). We discuss the results in §3 and summarize our conclusions in §4.

2 Observations and Analysis

The observations analyzed for this study are listed in Tables 1 (aimpoint), 2 ($\pm 10'$ off-axis) and 3 ($\pm 20'$ off-axis). Level 2 event lists were acquired from the *Chandra Data Archive*, and counts in source regions were measured using *funcnts*. Source and background regions were carefully chosen to represent the different source size and shape at each detector location. Source circle radii chosen for aimpoint, $10'$, and $20'$ analyses were 20 pixels, 50 pixels, and 100 pixels, respectively. The aimpoint source region accounts for $>99\%$ of the PSF. The $10'$ and $20'$ off-axis source regions account for the PSF core only ($<50\%$). In particular, the very large and distorted PSF of the $20'$ positive (+Y) wing data falls on the plate edge, limiting our analysis to just the core. For this reason, we recommend below (§4) that these data be acquired at a larger offset of $25'$. Background regions for the 3 data sets were chosen as an annulus with radii of 50 and 120 pixels around the aimpoint source, and a circular region with a radius of 500 pixels nearby the $10'$ and $20'$ off-axis sources. We calculated the background-subtracted count rate per observation and monitored over time. Exposure times were corrected by the average dead-time correction, given by the keyword *DTCOR* in the event list header.

In Figures 1 (aimpoint), 2 ($\pm 10'$ off-axis) and 3 ($\pm 20'$ off-axis), we show the evolution of the Vega/HRC-S count rates over the course of the *Chandra* mission to date. The mean count rate (dashed line) for all observations and standard deviation of the mean (dotted lines) are computed for each data set. We note that the $10'$ and $20'$ observations fall on thin filter portions of the HRC-S UVIS and therefore have much higher count rates than the aimpoint observations for equal exposure times. The background rate and the average dead-time correction factor per observation are also shown. Vertical lines indicate the start-dates at which the HRC door was left open during radiation zone passage and the implementation of improved dead-time calculations with *DS7.3*.

Michael Juda also maintains an independent webpage to monitor the health of the HRC UVIS (see Juda 2004b).

3 Results

Figures 1–3 suggest that there has been no obvious change over time with the HRC-S UV response. The apparent upward trend in count rate observed in the wing data is most likely an artifact of dead-time having been calculated incorrectly in earlier times. Vega is a stable UV source (variations $<8\%$ in bolometric luminosity) such that the wing observations are dominated by the source, practically eliminating the effects of background. Therefore, we expect the correctly calculated dead-time to be roughly the same for all observations. Additionally, nominal exposure times per observation before dead-time corrections are roughly the same (~ 3000 sec). For comparison, we over-plot in Figure 3 the wing data without the dead-time corrections applied (small symbols), and find a more level relationship with time.

The most recent wing plate observations, those with the most accurate dead-time corrections, all have very short exposure times relative to nominal. This indicates extreme telemetry saturation on the wings (*DTCOR* $\sim 65\%$), which we expect to be the case for all wing observations. We also

observe at least some saturation on the center plate at $-10'$ off-axis, with $DTCOR \sim 10-15\%$. Dead-time corrections will be improved and made more consistent upon completion of reprocessing of the entire *Chandra Data Archive*, scheduled to take place in 2005. Until then, too much uncertainty is introduced by the incorrectly calculated dead-times for most of the observations. Therefore, though it is not likely, we cannot rule out the possibility of UVIS damage due to the HRC remaining active during radiation zone passage. Further monitoring of the HRC-S UV response is required.

3.1 Non-Poisson Scatter

The Poisson statistical errors in the individual observations are small for the aimpoint, and very small for the $10'$ and $20'$ pointings. The data sets, however, show somewhat more scatter than simple Poisson statistics would allow. Some factors contributing to the added noise are listed below:

1. **Intrinsic source variability.** Vega is known to have a subtle δ Sct type variability, with m_V ranging from -0.02 to $+0.07$ (see Samus et al. 2004). This corresponds to flux variations of $\approx 8\%$ and is similar in magnitude to the count-rate standard deviation seen for aimpoint and $\pm 10'$ off-axis data. The maximal deviations seen in these data are however much larger than this, and in any case the $\pm 20'$ off-axis data show even larger deviations.
2. **Incorrect dead-time correction factors.** For all observations processed prior to *Data Systems* version *DS7.3* (implemented \sim July 2004) the instrument dead-time was calculated incorrectly. These would be especially pertinent on the wing plates. The telemetry saturation limit for the HRC-S is ~ 180 ct s^{-1} , which is easily achieved on the outer plates, which are covered with thinner filters and thus have larger backgrounds. This makes it difficult to separate dead-time effects and changes in UV response, and precludes a definitive conclusion. An effort to correctly account for dead-time effects is underway; here we simply note the lack of evolution in the background counts on the wing plates and take that as an indication that the true dead-time remains stable (see also Juda 2004b). We show the effects of ignoring dead-time corrections in Figure 3.
3. **Dither pattern coverage sampling QE spatial variations.** The exposure times of the observations span $\sim 800-3200$ seconds, which are comparable to the ~ 1100 seconds it takes for the dither to complete 1 cycle. The dither amplitude of ~ 300 pixels is significantly larger than the source regions, particularly on the center plate. Variations of duration and where the dither begins and ends could lead to sampling different regions of the detector with different QE responses, resulting in the observed scatter. It has been shown previously that QE varies on fairly small spatial scales, with the variation being more significant for low energy sources (see *CXC Memo* by Pease et al. 2004a; and Pease et al. 2004b, web-memos supporting HRC-S “Flat Field” calibration).
4. **Gain variations over time.** Finally, it has been shown that the HRC-S gain has been decaying with time (Pease & Drake 2003, and Posson-Brown & Donnelly 2003). Though the impact has not yet lead to significant loss of source X-rays below the lower-level discriminator, the effect resulting in QE “sag” should be greater for UV photons than X-rays, and needs to be taken into account for all HRC-S UV analyses. The largest gain decrease has occurred at the aimpoint ($\sim 25\%$). In Figure 4 we show the PHA distribution at the aimpoint for UV rays from Vega over-plotted with X-rays from AR Lac, both recent observations, acquired in February 2005.

4 Conclusions

We have analyzed all of the HRC observations of Vega obtained thus far. In order to avoid the plate gap, we recommend that the wing plate off-axis positioning be changed to 25'.

We do not find conclusive evidence for degradation of the UVIS, either over the long term, or since the time it was decided to leave open the HRC door during radiation-zone passages (though there are apparent trends in the latest observations – e.g., at the aim-point – which, while not statistically significant, must be monitored closely). Thus, we conclude that there has been no damage to the UVIS. However, we note that the HRC UVIS is now being exposed to a flux of low-energy particles which may yet lead to its degradation. Therefore, following Juda (2004a), we recommend the higher frequency (quarterly) schedule of observations, which will allow us to spot any degradation early and decide on a course of action.

5 References

1. Juda, M., 2004a, “HRC -Y Shutter Failure (OCCcm06110): FDB Closeout”, *Chandra Flight Note (#441)*
hea-www.harvard.edu/~juda/memos/shutter_anomaly/shutter_failure.pdf
2. Juda, M., 2004b, “Monitoring the UV/Ion-Shield Health”, *CXC Web-Memo*
hea-www.harvard.edu/~juda/memos/uvis_monitor/index.html
3. Pease, D., et al., 2004a, “Improvements to the HRC-S QE uniformity and LETGS effective area”, *CXC Calibration Workshop*
asc.harvard.edu/ccw/proceedings/04_proc/presentations/pease/
4. Pease, D., et al., 2004b, “HRC Flat Field Maps: HRC-S”, *CXC Calibration Web-Memo*
cxc.harvard.edu/cal/Hrc/flatfield.html#hrc-s
5. Pease, D., Drake, J., 2003, “Monitoring the HRC-S Gain with the LETG/HRC-S”, *CXC Calibration Memo*
cxc.harvard.edu/cal/Letg/Hrc_gain/
6. Posson-Brown, J., Donnelly, R.H., 2003, “Evolution of PHA Response in the HRC”, *CXC Calibration Memo*
cxc.harvard.edu/cal/Hrc/gain.html
7. Samus, N.N., Durlevich, O.V., et al., 2004, “Combined General Catalog of Variable Stars (GCVS4.2, 2004 Ed.)”
<http://vizier.u-strasbg.fr/viz-bin/Cat?II/250>

Table 1: HRC-S Observations of Vega: Nominal Aimpoint (Central MCP)

ObsID	Date	Exposure (s)	Net Counts	Error	BG Counts	DTCOR
01416	Oct99	3106.32	501.3	22.6	229.	0.99812
00032	Jun00	2891.60	465.5	21.7	194.	0.99994
00988	Feb01	2349.45	348.9	18.8	153.	0.99995
00989	Aug01	2353.54	408.7	20.4	158.	0.99995
02589	Feb02	2817.83	434.0	21.0	179.	0.99922
03688	Jan03	1845.21	270.5	16.6	163.	0.99998
05051	Feb04	1841.13	283.3	17.1	228.	0.99943
05343	Aug04	3269.81	429.0	20.9	208.	0.99464
05347	Nov04	3129.67	422.4	20.7	225.	0.99287
05966	Feb05	2140.62	313.6	17.9	161.	0.99436

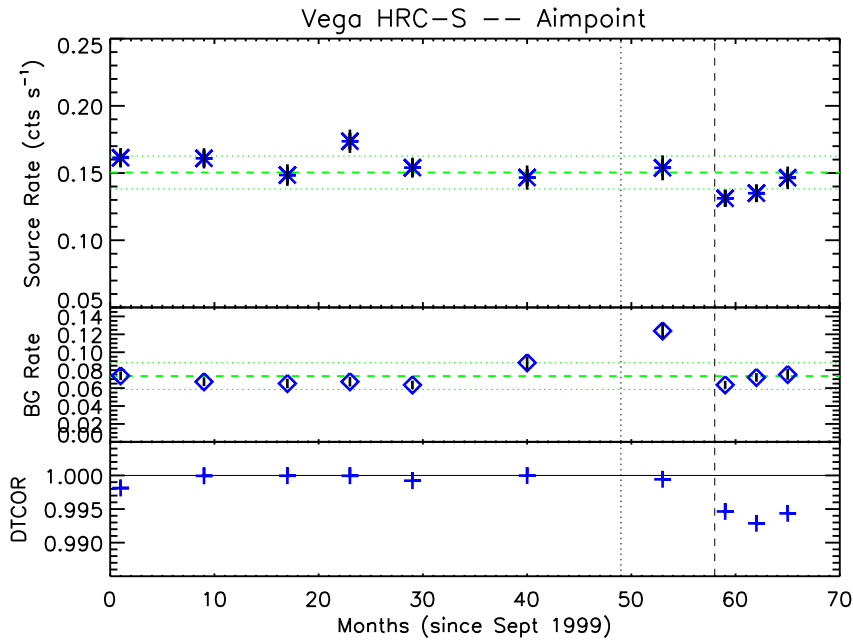


Figure 1: HRC-S UV rates, background rates, and dead-time corrections for Vega observations at nominal aimpoint on center MCP. Also shown are the sample mean μ (dashed line) and standard deviation σ (dotted lines) for the observed rates. The maximal variation is 28% around the mean, and $\sigma/\mu = 0.08$. Vertical lines indicate start-date of HRC door staying open during radiation zone passage (October 2003 - dotted) and implementation of DS7.3 (July 2004 - dashed).

Table 2: HRC-S Observations of Vega: $\pm 10'$ off-axis(Central MCP)

ObsID	Date	Exposure (s)	Net Counts	Error	BG Counts	DTCOR
negative direction						
00990	Feb01	2454.67	205915.	453.8	1767.	0.909
00991	Aug01	2423.52	187402.	432.9	1823.	0.899
02590	Feb02	2931.44	246297.	496.3	2030.	0.919
03689	Jan03	1956.92	167344.	409.1	2114.	0.914
05052	Feb04	1826.83	131981.	363.3	3496.	0.853
05967	Feb05	1888.30	168002.	409.9	1588.	0.874
positive direction						
01417	Oct99	3202.51	232347.	482.0	1801.	0.9997
01805	Aug00	2820.75	259811.	509.7	1296.	0.9999

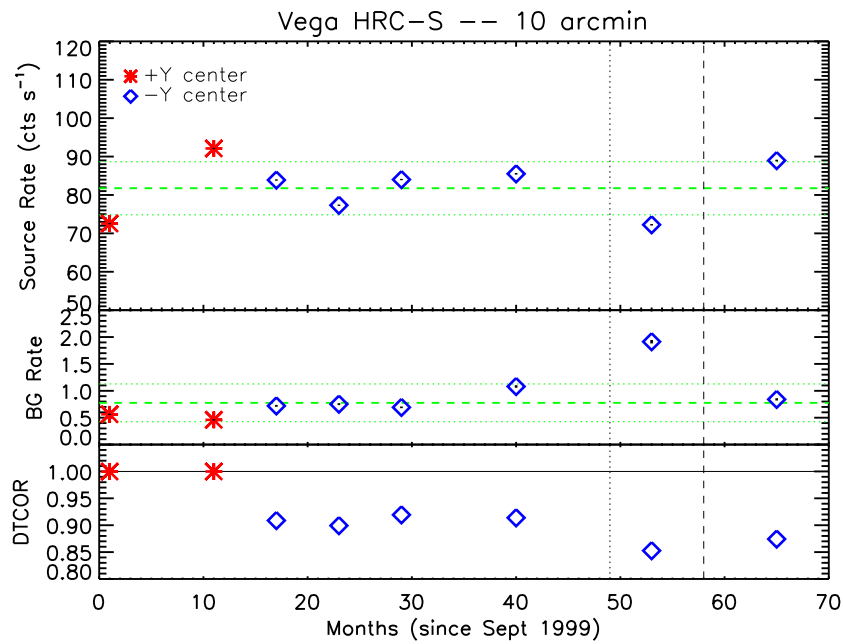


Figure 2: HRC-S UV rates, background rates, and dead-time corrections (as in Figure 1) for Vega observations at $\pm 10'$ off-axis on center MCP. For these data, the maximal variation is 24% around the sample mean, and $\sigma/\mu = 0.085$.

Table 3: HRC-S Observations of Vega: $\pm 20'$ off-axis (Wing MCPs)

ObsID	Date	Exposure (s)	Net Counts	Error	BG Counts	DTCOR
negative wing						
00992	Feb01	2554.67	116237.	341.0	799.	0.950
00993	Aug01	2653.83	111576.	334.1	723.	0.986
02591	Feb02	1749.84	130590.	361.4	846.	0.568
03690	Jan03	1149.99	86322.	293.9	648.	0.537
05053	Feb04	1243.04	76807.	277.2	1394.	0.580
05345	Aug04	1122.68	105386.	324.8	3021.	0.341
05349	Nov04	1199.99	128494.	358.5	1104.	0.376
05368	Feb05	854.82	81928.	294.6	610.	0.391
positive wing						
01418	Oct99	3197.32	117416.	342.7	734.	0.998
01806	Aug00	2717.27	129562.	360.0	580.	0.855
05344	Aug04	1161.45	123002.	350.8	973.	0.354
05348	Nov04	1108.56	129228.	359.5	1003.	0.349
05369	Feb05	777.98	86740.	294.6	527.	0.355

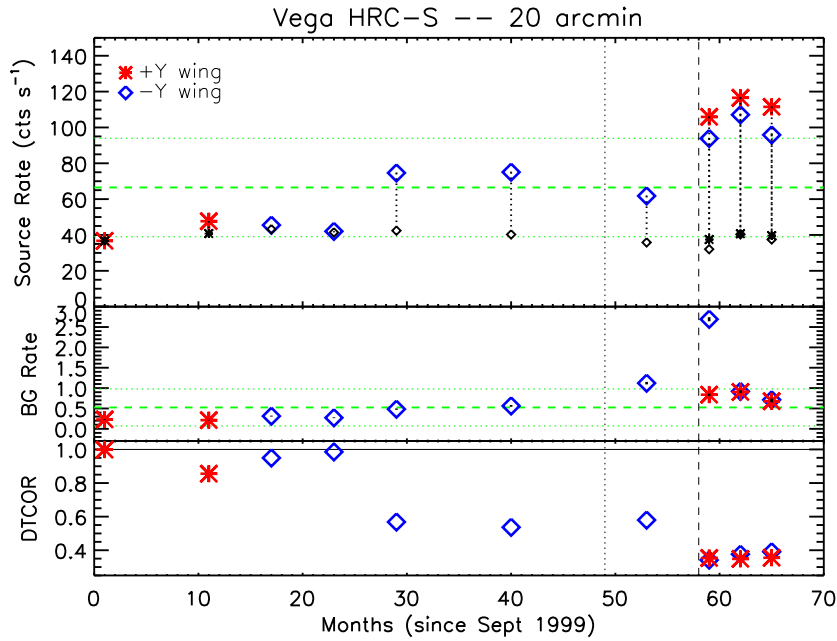


Figure 3: HRC-S UV rates, background rates, and dead-time corrections (as in Figure 1) for Vega observations at $\pm 20'$ off-axis on wing MCPs. For these data, the maximal variation is 120% around the sample mean, and $\sigma/\mu = 0.41$. The rates calculated both including dead-time corrections (larger symbols) and excluding it (smaller symbols) are shown, with vertical lines joining the two. Note the large effects due to the dead-time corrections.

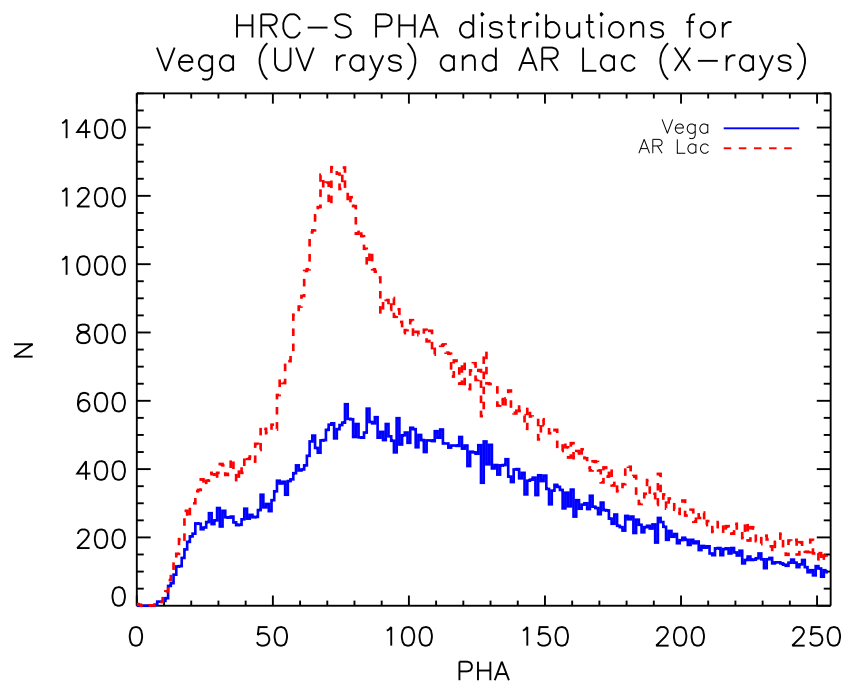


Figure 4: HRC-S PHA distributions for UV rays from Vega (solid histogram) over-plotted with X-rays from AR Lac (dashed histogram). Both data were acquired in February 2005.